The American Journal of Pathology, Vol. 169, No. 6, December 2006

DOI: 10.2353/ajpath.2006.060475

Cardiovascular, Pulmonary and Renal Pathology

Phenyl-α-*tert*-Butyl Nitrone Reverses Mitochondrial Decay in Acute Chagas' Disease

Jian-Jun Wen,* Vandanajay Bhatia,*
Vsevolod L. Popov,† and Nisha Jain Garg*†

From the Departments of Microbiology and Immunology and Pathology,† University of Texas Medical Branch, Galveston, Texas*

In this study, we investigated the mechanism(s) of mitochondrial functional decline in acute Chagas' disease. Our data show a substantial decline in respiratory complex activities (39 to 58%) and ATP (38%) content in *Trypanosoma cruzi*-infected murine hearts compared with normal controls. These metabolic alterations were associated with an approximately fivefold increase in mitochondrial reactive oxygen species production rate, substantial oxidative insult of mitochondrial membranes and respiratory complex subunits, and >60% inhibition of mtDNA-encoded transcripts for respiratory complex subunits in infected myocardium. The antioxidant phenyl-α-*tert*-butyl nitrone (PBN) arrested the oxidative damage-mediated loss in mitochondrial membrane integrity, preserved redox potential-coupled mitochondrial gene expression, and improved respiratory complex activities (47 to 95% increase) and cardiac ATP level (≥40% increase) in infected myocardium. Importantly, PBN resulted twofold decline in mitochondrial reactive oxygen species production rate in infected myocardium. Taken together, our data demonstrate the pathological significance of oxidative stress in metabolic decay and energy homeostasis in acute chagasic myocarditis and further suggest that oxidative injuries affecting mitochondrial integrity-dependent expression and activity of the respiratory complexes initiate a feedback cycle of electron transport chain inefficiency, increased reactive oxygen species production, and energy homeostasis in acute chagasic hearts. PBN and other mitochondria-targeted antioxidants may be useful in altering mitochondrial decay and oxidative pathology in Chagas' disease. *(Am J Pathol 2006, 169:1953–1964; DOI: 10.2353/ajpath.2006.060475)*

Chagas' disease is a pathological process induced by infections with the hemoflagellate protozoan *Trypanosoma cruzi* and is a major human health problem in the southern parts of the American continent.[1] In >95% of acutely infected individuals, parasitemia is controlled by the immune system. After several years of a clinically silent but ongoing process of organelle and myocardial degeneration, >40% of seropositive patients develop chronic cardiomyopathy.

Since early findings of abnormal mitochondria in cardiac biopsies obtained from seropositive patients,[2] mitochondrial impairment has been associated with cardiac dysfunction in Chagas' disease. Quantitative light and electron microscopic analysis of the myocardial biopsy samples from human chagasic patients and experimental models has revealed that mitochondrial degenerative changes occur early in the course of *T. cruzi* infection and are exacerbated with progressive disease severity.[2–5] The functional decline of cardiac mitochondria in experimental models of Chagas' disease was shown by impaired activities of the respiratory complexes that contain subunits encoded by mtDNA and nDNA.[6–8] The demonstration of inefficient ATP production in infected mice[8] provided the first indication of the physiological effects of mitochondrial dysfunction in chagasic hearts.

Toward understanding the mechanism(s) of mitochondrial decay, it is important to note that mitochondria are exposed to consistent oxidative stress in chagasic hearts. *T. cruzi* infection elicits host immune responses.[9] These immune mechanisms control parasite burden in infected host through release of reactive oxygen species (ROS) and reactive nitrogen species.[9,10] In the heart, superoxide anions (O_2^-) are produced as a by-product of mitochondrial electron transport chain.[11] This mitochondrial reactive oxygen species (mtROS) generation can increase exponentially when the electron transport chain functions at a suboptimal level[12,13] and might be the case in infected myocardium consisting of impaired activity of CI and CIII respiratory complexes.[8] It is, thus, likely that ROS-mediated responses, through various interrelated

Supported in part by the National Institutes of Health (grants AI053098 and AI054578 to N.J.G.).

Accepted for publication September 1, 2006.

Address reprint requests to Dr. Nisha Jain Garg, 3.142C Medical Research Building, University of Texas Medical Branch, 301 University Blvd., Galveston TX 77555. E-mail: nigarg@utmb.edu.

mechanisms, may contribute to a mitochondrial functional decline in chagasic hearts. For example, free radical-mediated oxidation of mitochondria, as noted in infected myocardium,[14] can affect mitochondrial biogenesis,[15–17] integrity,[18] and/or gene expression.[19] Oxidative modifications of mitochondrial membranes can result in the opening of the mitochondrial permeability transition pores and dissipation of the proton gradient, essential for the efficient transfer of electrons through the electron transport chain and ATP formation.[20,21] The mtDNA is particularly susceptible to oxidative damage and, if not repaired properly, can lead to mtDNA mutation and/or depletion that would affect the expression and assembly of respiratory complexes, and, subsequently, the electron transport chain efficiency.[22–25] These mechanisms, however, remain to be delineated in chagasic myocarditis.

Phenyl-*N-tert*-butylnitrone (PBN), a nitrone-based compound, is a potent antioxidant. PBN has been shown to 1) trap or scavenge a wide variety of free radical species, including biologically relevant $O_2^{\cdot-}$ and hydroxyl (OH•) radicals; 2) increase endogenous antioxidant levels; and 3) inhibit free radical generation.[26] In addition, PBN has been shown to inhibit the expression of a variety of inflammation-associated gene products.[27] In this study, we treated mice with PBN to determine whether increasing the antioxidant capacity would arrest oxidative stress and positively alter mitochondrial function in the myocardium of infected mice. We discuss the mechanisms of action of PBN in protecting the acute chagasic myocardium from mitochondrial dysfunction-associated energy (ATP) homeostasis.

Materials and Methods

Mice and Parasites

Six- to 8-week-old male C3H/HeN mice were purchased from Harlan (Indianapolis, IN). *T. cruzi* trypomastigotes (SylvioX10/4 strain) were maintained and propagated by the continuous *in vitro* passage of parasites in monolayers of C2C12 cells[28] and used for infection of mice (10,000/mouse, intraperitoneal). Mice were given PBN (50 mg/kg) by intraperitoneal injection on alternate days throughout the course of infection. Mice were sacrificed in acute infection phase (27 to 35 days after infection). Animal experiments were performed according to the National Institutes of Health Guide for Care and Use of Experimental Animals and approved by the University of Texas Medical Branch Animal Care and Use Committee.

DNA and RNA Isolation

Heart tissue sections (50 mg) were finely chopped and incubated for 4 hours at 55°C in 250 μl of lysis buffer [50 mmol/L Tris-HCl, pH 7.5, containing 0.5% sodium dodecyl sulfate, 10 mmol/L ethylenediaminetetraacetic acid (EDTA), 0.1 mol/L NaCl, and 400 μg/ml proteinase K]. Tissue lysates were extracted twice with an equal volume of phenol/chloroform/isoamylalcohol (24:24:1), and total DNA was purified by ethanol precipitation. All DNA samples were suspended in 100 μl of distilled H_2O.[5]

For RNA isolation, freshly excised hearts were cut into pieces, blotted onto paper towels to remove excess blood, and flash-frozen in liquid nitrogen. The frozen tissues were individually transferred into guanidine-phenol solution and processed with a tissue homogenizer, and the total RNA was isolated as described.[29,30] Total RNA was resolved by denaturing formaldehyde gel electrophoresis, quantitated, and stored at −80°C.

Mitochondria Isolation

Heart tissue sections were homogenized in 20 mmol/L Tris-HCl at pH 7.4, containing 250 mmol/L sucrose, 2 mmol/L K_2EGTA [tissue/buffer ratio, 1:10 (w/v)], and cardiac mitochondria isolated by differential centrifugation.[8] When tissue samples were processed for estimation of protein carbonyls and thiobarbituric acid-reactive substances, extraction buffer included 2% β-mercaptoethanol and 500 μmol/L butylated hydroxytoluene, respectively.

Parasite Detection

For parasite detection, polymerase chain reaction (PCR) was performed for 28 cycles, using *T. cruzi* 18S rDNA-specific oligonucleotides[5] with 2 μl of the total DNA as template. Denaturation, annealing, and elongation steps were performed for 1 minute each at 94°C, 58°C, and 72°C, respectively. A 5-μl aliquot of each PCR reaction was resolved on a 1.2% agarose gel. The ethidium bromide-stained gels were visualized using long-wave UV light and densitometric analysis performed on a FluorChem Imaging System (Alpha Innotech, San Leandro, CA).

Mitochondrial DNA and mRNA Levels

The mtDNA content in infected murine hearts was examined by Southern blot analysis.[8] In brief, total DNA samples were digested with *Bam*HI restriction enzyme, resolved on 1% agarose gel, and transferred to Zeta-Probe membrane (Bio-Rad, Hercules, CA). Membranes were hybridized with ^{32}P-labeled *CO2* cDNA probe and exposed to a phosphorimaging screen. The images were captured using a Storm 860 PhosphorImager (Molecular Dynamics, Sunnyvale, CA) and densitometric analysis was performed. After stripping off the *CO2* probe, the same membranes were hybridized with a β-actin probe.

We examined mitochondrial gene expression by Northern blot analysis.[8] Total RNA samples were resolved on 1% agarose gel containing 2 mol/L formaldehyde and transferred to the Zeta-Probe membrane. Membranes were hybridized with ^{32}P-labeled cDNA probes (*ND4L*, *CO1*, *CO2*, *ATP6*, *ATP8*)[8] and the images captured and analyzed, as above. All cDNAs used as probe were amplified by reverse transcriptase (RT)-PCR using gene-specific primer pairs and total RNA isolated from C57BL/6 mouse as template. The cDNA amplicons were

cloned in Topo (T) vector and confirmed by restriction digestion and sequencing at a University of Texas Medical Branch core facility.[8]

Real-Time RT-PCR

First-strand cDNA was synthesized from total RNA (2 μg) using 2.5 U of Superscript II reverse transcriptase and 1 μmol/L poly(dT)$_{18}$ oligonucleotide at 42°C for 50 minutes in a 20-μl reaction volume. Real-time PCR reactions (25-μl volume) were performed in an iCycler thermal cycler (Bio-Rad) using SYBR-Green Supermix (Bio-Rad) with 2 μl of the 10-fold diluted cDNA and 5 μl of 1 μmol/L primer pair specific for antioxidant cDNAs[31] and mitochondria-encoded genes.[8] The PCR base line subtracted curve fit mode was applied for threshold cycle (C_t) determination, using iCycler iQ real-time detection system software, version 3.0a (Bio-Rad). For each target gene, the C_t values were normalized to *GAPDH* expression and represent the mean of triplicate samples in two independent experiments. The relative expression level of each target gene in infected mice was calculated using the formula fold change = $2^{-\Delta Ct}$, where ΔC_t represents the C_t (infected sample) $-$ C_t (control). To visualize better the mRNA levels in all groups, bar graphs were generated by plotting the $1/2^{Ct}$ values on the *y* axis.[32]

Respiratory Complex Activities

Cardiac mitochondria were isolated in 5 mmol/L HEPES at pH 7.2, containing 210 mmol/L mannitol, 70 mmol/L sucrose, 1 mmol/L EGTA, and 0.1% fatty acid-free bovine serum albumin. The activities of the respiratory complexes (CI, CII, and CIII) and citrate synthase were monitored by spectrophotometric methods as described.[8,33] Total protein was measured using the Bradford assay[34] and specific activities evaluated using extinction coefficients: CI, ε5.5 mmol/L$^{-1}\cdot$cm^{-1}; CII and CIII, ε19.1 mmol/L$^{-1}\cdot$cm^{-1}; citrate synthase, ε13.6 mmol/L$^{-1}\cdot$cm^{-1}. The specificity of the enzyme reactions was determined by monitoring changes in absorbance in the presence of specific inhibitors (CI, 6.5 μmol/L rotenone; CIII, 5 μg/ml antimycin). In some experiments, respiratory complexes were resolved by blue native-polyacrylamide gel electrophoresis (BN-PAGE),[35] and enzymatic activities determined by in-gel catalytic staining.[8,36] Gel images were visualized and analyzed on a FluorChem 8800.

Lipid and Protein Oxidation

We measured lipid peroxidation products, ie, malonyldialdehydes, by using a biochemical assay of thiobarbituric acid-reactive substances (ε1.56 $\times$ 10^5 mol/L^{-1} cm^{-1}), described previously.[37,38] To estimate the protein oxidation level, cardiac mitochondria samples were incubated with 2,4-dinitrophenylhydrazine and DNP-derivatized carbonylated proteins detected by Western blotting with anti-DNP antibody.[8,39] The carbonylated subunits of the mitochondrial respiratory complexes were detected by two-dimensional BN-PAGE/Western blotting with anti-DNP antibody.[14,35] After Western blot analysis, membranes were stained with 0.005% Coomassie blue G250 (Bio-Rad).

Glutathione Content

Glutathione content was determined by a DTNB-GSSG reductase recycling assay,[38,40] modified for 96-well plates.[41]

ATP Content

Freshly harvested cardiac tissue samples were homogenized in 50 mmol/L Tris-HCl at pH 7.2, containing 100 mmol/L KCl, 5 mmol/L $MgCl_2$, 1.0 mmol/L EDTA, and 2% TCA [tissue/buffer, 1:10 (w/v)]. Tissue homogenates were suspended in prewarmed (95°C) extraction buffer (100 mmol/L Tris at pH 7.75, containing 4 mmol/L EDTA) (1:9 v/v) and incubated in a boiling water bath for 2 minutes. After cooling on ice, tissue extracts were centrifuged at 1000 $\times$ *g* for 1 minute, and the supernatant used to measure ATP content.[42] Mitochondria isolated from fresh tissues were used immediately for ATP content determination.

ATP content was monitored by a firefly luciferase method[42] using a Veritas microplate luminometer (Promega, Madison, WI). In brief, 160 μl of ATP-monitoring reagent, consisting of 15 mmol/L potassium phosphate at pH 7.0, 150 mmol/L sucrose, 2 mmol/L $Mg(CH_3COO)_2$, 0.5 mmol/L EDTA, 2.5 μg/ml luciferase, 20 μg/ml D-luciferin, and 0.5 mg/ml bovine serum albumin, was distributed in black-bottomed 96-well plates. After 5 minutes of incubation, 40-μl samples in 10-fold dilutions (1:1000 to 1:20,000) were added, and the change in absorbance monitored for 30 minutes. The standard curve was prepared with purified ATP (linear range, 25 pmol/L to 25 nmol/L; Sigma, St. Louis, MO).

H_2O_2 Content

Freshly prepared heart homogenate or isolated mitochondria samples were suspended in P buffer (10 mmol/L Tris-HCl at pH 7.4, 250 mmol/L sucrose, and 1 mmol/L EDTA), and added in triplicate (50 μg protein/50 μl/well), to 96-well, flat-bottomed plates. The reaction was started, in the dark, by adding 50 μl of 100 μmol/L Amplex Red (10-acetyl-3,7-dihydroxyphenoxazine; Invitrogen, Carlsbad, CA), and 50 μl of 0.3 U/ml horseradish peroxidase per well.[13] In the presence of horseradish peroxidase, Amplex Red reacts with H_2O_2 in 1:1 stoichiometry, resulting in the formation of red fluorescent resorufin that was estimated at absorption and fluorescence emission maxima of 567 and 587 nm, respectively, using a Spectra Max M2 microplate reader (Molecular Devices). For the estimation of H_2O_2 generation rate, mitochondria were incubated in presence of complex II (succinate) substrate, and H_2O_2 formation monitored for

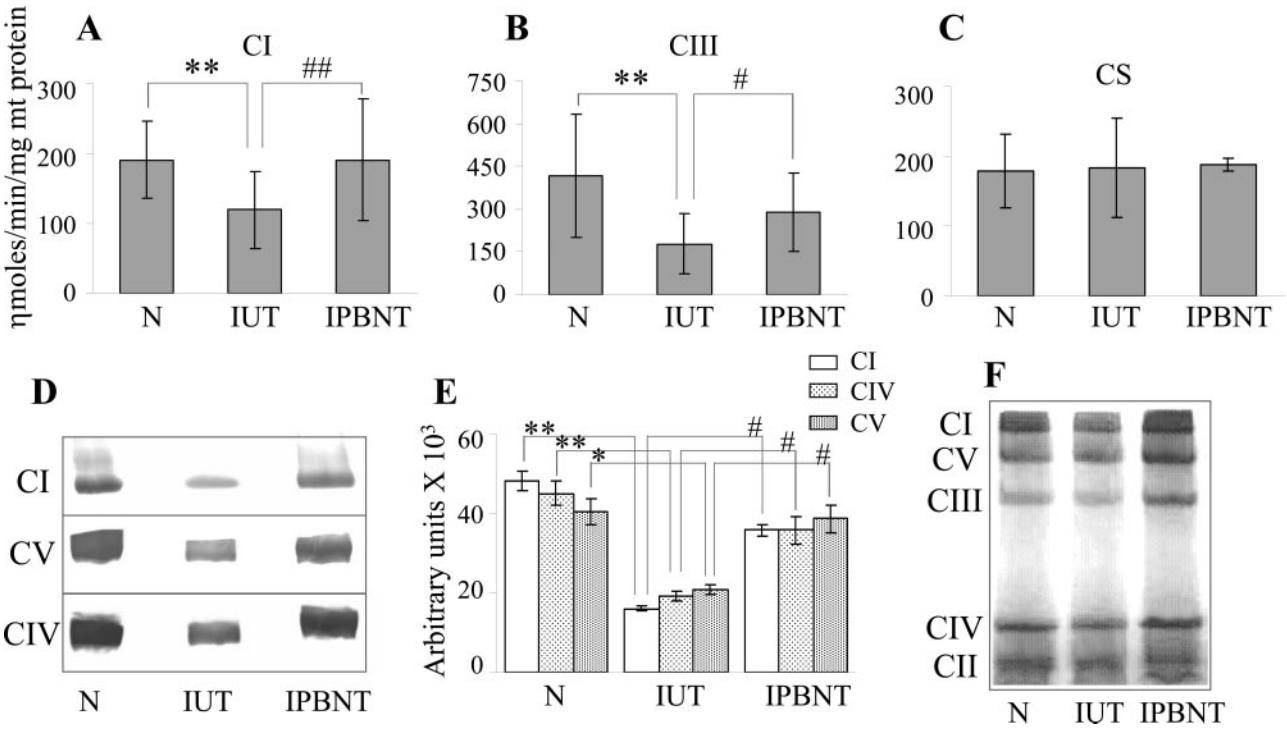

Figure 1. Myocardial respiratory complex activities in *T. cruzi*-infected (±PBN) mice. Shown are the specific activities of CI (**A**) and CIII (**B**) respiratory complexes and citrate synthase (**C**) in cardiac mitochondria of normal (N), infected/untreated (IUT), and infected/PBN-treated (IPBNT) mice, measured by spectrophotometric methods. Histochemical staining. Respiratory complexes of cardiac mitochondria were resolved by BN-PAGE. The BN gels were processed by either staining the whole gel with Coomassie blue (**F**) or subjecting gel slices containing individual complexes to enzymatic colorimetric reactions (**D**). Densitometric quantitation of catalytic staining for each respiratory complex was normalized to a Coomassie-stained complex (**E**). The data (mean ± SD) are representative of three independent experiments ($n = 3$ per experiment/group). $^{**\#\#}P < 0.01$; $^{*\#}P < 0.05$.

60 minutes. The standard curve was prepared with purified H_2O_2 (linear range, 50 nmol/L to 5 μmol/L).

Histology

The heart tissues were removed and fixed in 10% buffered formalin for 24 hours, dehydrated in absolute ethanol, cleared in xylene, and embedded in paraffin. Sections (5 μm) were stained with hematoxylin and eosin and evaluated by light microscopy. Tissues were scored 0 to 4 in blind studies according to the extent of inflammation and tissue damage from normal to total wall involvement.[43,44]

Electron Microscopy

After infection, heart tissue from infected mice were harvested and fixed in modified Ito's fixative (2.5% formaldehyde, 0.1% glutaraldehyde, 0.03% $CaCl_2$, and 0.03% trinitrophenol in 0.05 mol/L cacodylate buffer, pH 7.3) at room temperature for 1 hour and then overnight at 4°C. After washing, samples were postfixed in 1% osmium tetraoxide for 1 hour and *en bloc* stained with 2% aqueous uranyl acetate. After dehydration in a graded series of ethanol, samples were embedded in Poly/Bed 812 (Polysciences, Warrington, PA). Ultrathin sections were cut on a Sorvall MT-6000 ultramicrotome, stained with lead citrate, and examined in a Philips 201 transmission electron microscope (Philips Electron Optics, EI Co., Hillsboro, OR) at 60 kV.

Data Analysis

The results are presented as the mean ± SD and were derived from at least triplicate observations per sample ($n \geq 9$ animals/group). The statistical significance was determined by Student's *t*-test. The level of significance between infected versus normal mice is presented by $P < 0.05$. The level of significance between infected/PBN-treated versus infected/untreated mice is presented by $P < 0.05$.

Results

PBN Improved the Mitochondrial Inefficiency of Respiratory Chain in the Myocardium of T. cruzi*-Infected Mice*

We evaluated the mitochondrial respiratory complex activities by a spectrophotometric method (Figure 1, A and B; Table 1). The myocardium of infected mice exhibited 39 and 58% decline in CI and CIII respiratory complex activities, respectively, when compared with those in normal controls ($P < 0.01$). PBN treatment resulted in a 95 and 47% inhibition of the myocardial loss of CI and CIII

Table 1. PBN Treatment Arrested the Mitochondrial Decay in Acute Chagasic Hearts

Parameters	Normal (N)	Infected/untreated (IUT)	Infected/PBN-treated (IPBNT)
Cardiac mitochondria			
CI (nmol/minute/mg mt protein)	194.9 ± 54.4	119.7 ± 54.9**	190.9 ± 86.5††
CII (nmol/minute/mg mt protein)	212.9 ± 10.0	215.2 ± 12.7	204.8 ± 88
CIII (nmol/minute/mg mt protein)	417.4 ± 216.5	177.0 ± 105.1**	288.0 ± 136.8†
CS (nmol/minute/mg mt protein)	177.6 ± 53	184 ± 71	187 ± 9
ATP (nmol/mg mt protein)	484 ± 107.9	351 ± 47.1*	429.9 ± 38.5†
MDA (nmol/mg mt protein)	0.30 ± 0.04	0.63 ± 0.00**	0.26 ± 0.02††
H_2O_2 (pmol/mg mt protein)	588.37 ± 32.82	769.63 ± 7.25*	505.48 ± 91.82†
H_2O_2 (pmol/60 minutes/mg mt protein)	96.99 ± 0.81	513.56 ± 92.18*	282.26 ± 38.54†
Cardiac tissue			
ATP (nmol/mg cardiac protein)	27.46 ± 0.98	17.15 ± 0.32**	22 ± 2.03†
H_2O_2 (pmol/mg cardiac protein)	32.33 ± 0.23	70.34 ± 2.08**	76.73 ± 3.63
GSH (nmol/mg cardiac protein)	15.63 ± 1.93	11.91 ± 3.38*	14.73 ± 1.53

Mice were infected with *T. cruzi* ± PBN. Results shown are mean ± SD. CI, CII, and CIII represent respiratory complexes I, II, and III, respectively. CS, citrate synthase; MDA, malonylaldehyde; mt, mitochondria.
*The level of significance between N versus IUT mice.
†The level of significance between IUT versus IPNBT mice.
*†$P < 0.05$; **††$P < 0.01$.

activities, respectively, in infected mice ($P < 0.05$). Similar levels of citrate synthase (Figure 1C) and CII complex (Table 1) activities in all cardiac mitochondria samples extracted from normal and infected (±PBN) tissues confirmed the comparable efficiency of mitochondria isolation in different experiments.

Spectrophotometric analysis may also detect cellular activities that are not specific to mitochondrial respiratory complexes. To validate the spectrophotometry results, we performed histochemical staining of the individual respiratory complexes, resolved by BN-PAGE. The identity of the complexes was confirmed by immunoblot analysis using antibodies (Molecular Probes, Eugene, OR) to specific subunits, ie, 39-kd subunit of CI, 70-kd SDH subunit of CII, 29-kd Rieske iron-sulfur protein of CIII, 20-kd subunit IV of CIV, and 56-kd β subunit of CV (data not shown). The densitometric units (Figure 1E) for the catalytically stained area of each complex (Figure 1D) were normalized to the corresponding Coomassie-stained band intensity (Figure 1F). Catalytic staining revealed a 67, 48, and 58% decline in CI, CIV, and CV activities, respectively, in acutely infected murine hearts ($P < 0.05$). PBN treatment of infected mice resulted in a 62, 90, and 64% inhibition of the loss in myocardial CI, CIV, and CV activities, respectively ($P < 0.05$). The detection of similar sizes of complexes in all mice (Figure 1F) suggests that *T. cruzi*-mediated stress responses did not alter the assembly of the respiratory complexes in the cardiac mitochondria. Together, the spectrophotometric and histochemical staining show that PBN treatment was effective in arresting, at least partially, the deficiencies of respiratory complexes in the myocardium of infected mice.

Inhibition of respiratory complexes is likely to disturb electron transport chain efficiency, and may subsequently affect oxidative phosphorylation. We determined whether myocardial energy status was affected in infected mice and if PBN-mediated restoration of respiratory complex activities enhanced the cardiac energy level in infected mice. Our data show that myocardial ATP content in infected mice was decreased by 38% as compared with that of normal controls ($P < 0.01$). PBN resulted in 47% inhibition of the ATP loss in infected murine hearts ($P < 0.05$) (Figure 2A, Table 1). The gain in myocardial ATP content was associated with increased mitochondrial ATP levels. The cardiac mitochondrial ATP content in infected mice was decreased by 27% relative to that in controls ($P < 0.05$). PBN resulted in a 59% inhibition of loss of mitochondrial ATP contents in infected mice ($P < 0.05$) (Figure 2B, Table 1).

In addition to decreased energy output, electron transport chain inefficiency may also result in increased release of electrons to molecular oxygen and free radical

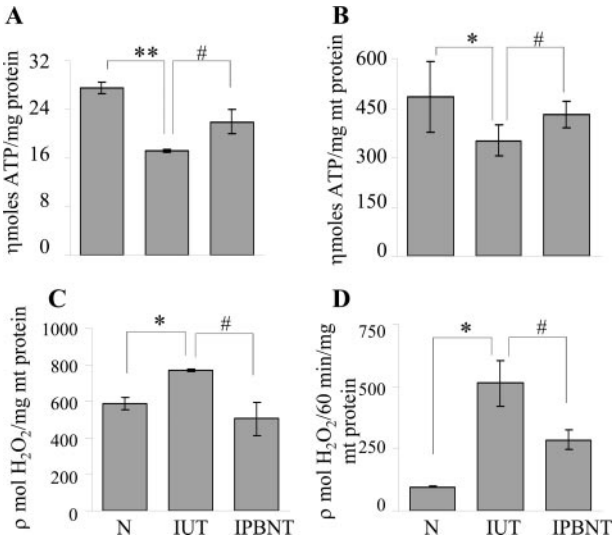

Figure 2. ATP content in *T. cruzi*-infected (±PBN) mice. Shown is the ATP content present in heart homogenates (**A**) and freshly isolated cardiac mitochondria (**B**) from normal (N), infected/untreated (IUT), and infected/PBN-treated (IPBNT) mice. H_2O_2 level in cardiac mitochondria of infected (±PBN) mice. **C:** Freshly isolated cardiac mitochondria were used to evaluate total H_2O_2 levels. **D:** Mitochondrial H_2O_2 release rate was measured in presence of complex II substrate (succinate). Data (mean ± SD) are representative of three independent experiments ($n = 3$ mice/experiment/group). **##$P < 0.01$; *#$P < 0.05$.

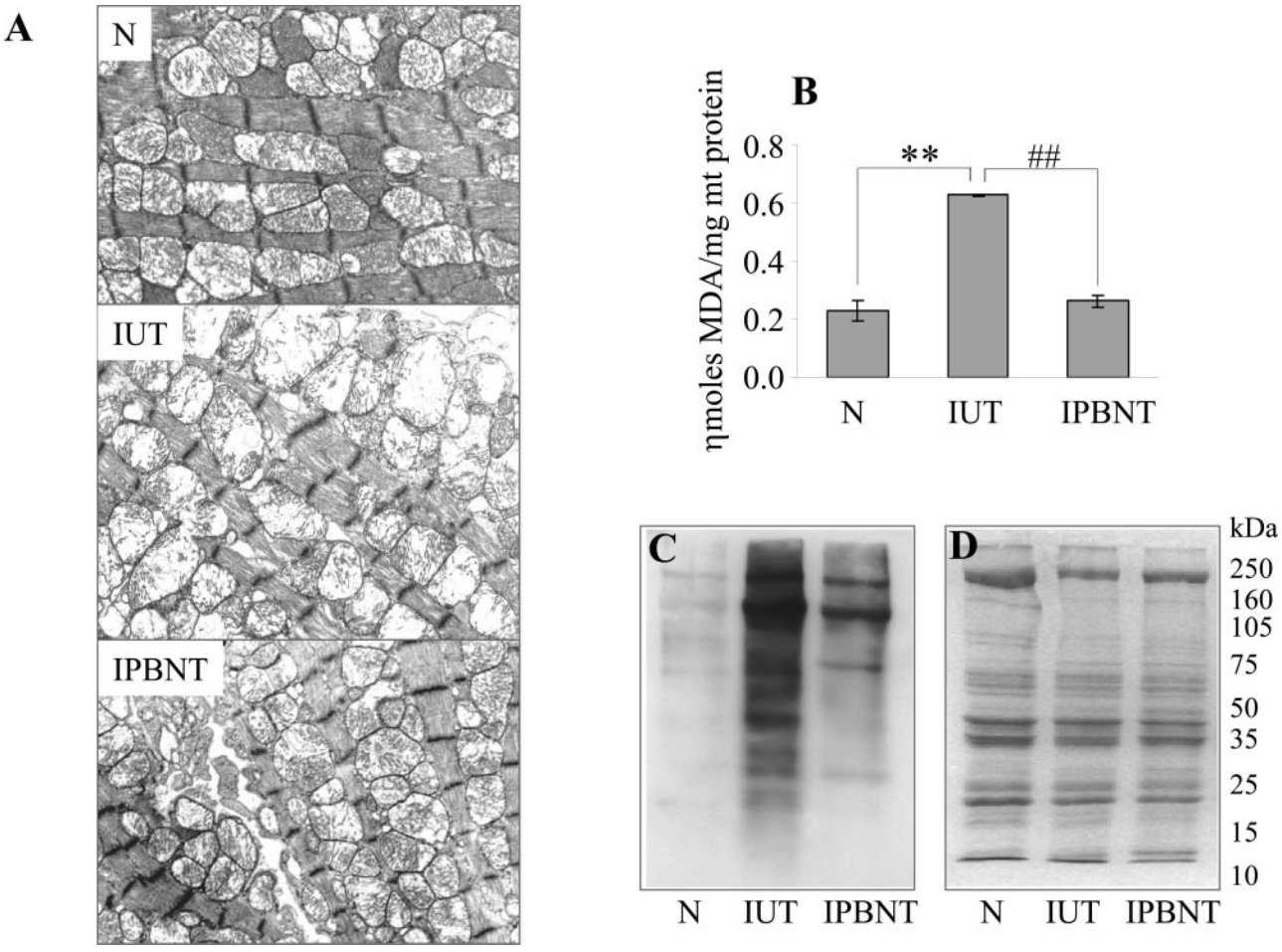

Figure 3. Transmission electron microscopy of heart tissue from *T. cruzi*-infected (±PBN) mice. **A:** Representative micrographs from ultrathin sections of heart tissue obtained from normal (N), infected/untreated (IUT), and infected/PBN-treated (IPBNT) mice are shown. Swollen mitochondria with extensive loss of cristae are presented in IUT. Note the absence of these features in cardiac myocyte of N and IPBNT mice. Oxidative modifications of cardiac mitochondrial membranes in infected (±PBN) mice. **B:** Lipid peroxidation products, ie, malonyldialdehydes, in cardiac mitochondria of acutely infected and infected/PBN-treated mice were compared by a thiobarbituric acid-reactive substance assay. **C:** Isolated cardiac mitochondria were derivatized with dinitrophenylhydrazide, and the DNP-reactive proteins identified by Western blot analysis. **D:** The results of Coomassie blue staining of the membrane used for Western blotting is shown. Data are representative of five independent experiments ($n = 3$ mice/group). $^{**\#\#}P < 0.01$. Scale bar = 1 μm. Original magnifications, ×14,100.

production.[11] We measured, using a redox-sensitive fluorescent dye, the mitochondrial H_2O_2 contents and H_2O_2 release rate. The mitochondrial H_2O_2 content, expressed as pmol/mg mt protein, was increased by 31% in infected mice compared with controls (Figure 2C, Table 1). This increase in mitochondrial H_2O_2 levels was associated with fivefold increase in the rate of mitochondrial H_2O_2 release in the myocardium of infected mice compared with that in normal controls ($P < 0.01$; Figure 2D, Table 1). On PBN treatment of infected mice, the mitochondrial H_2O_2 levels in the myocardium were normalized to that detected in controls (Figure 2C, Table 1) and was associated with twofold decline in the rate of H_2O_2 release compared with that detected in infected/untreated mice ($P < 0.01$; Figure 2D, Table 1). Together, these data suggest that electron transport chain inefficiency results in decreased energy output and increased oxidative stress in the myocardium of *T. cruzi*-infected mice and that PBN treatment is effective in improving the cardiac mitochondrial function in infected mice.

PBN Arrested the Oxidative Stress-Mediated Mitochondrial Decay in Infected Murine Hearts

Multiple, oxidative stress-mediated interrelated mechanisms can contribute to mitochondrial decay. For example, oxidation of mitochondrial membrane components may alter the mitochondrial integrity, and thus disturb the mitochondrial membrane potential that is essential for maintaining the efficient transfer of electrons through the electron transport chain and ATP formation. We examined in cardiac tissue of infected mice for the changes in mitochondrial morphology by transmission electron microscopic analysis and oxidation of mitochondrial membrane components, ie, derivatives of lipid peroxidation by thiobarbituric acid-reactive substances assay and DNP-derived carbonyl proteins by Western blotting. As shown in Figure 3A, heart tissue sections from infected/untreated mice (IUT) revealed severe mitochondrial morphological alterations; a majority of mitochondria were

large and swollen, and they lacked cristae, which are formed by the inner membrane. These changes were particularly evident when compared with heart tissue sections obtained from normal controls (Figure 3A, compare IUT versus N). Further, we observed that mitochondrial membrane components (lipids and proteins) were susceptible to ROS-induced oxidation in infected mice. Our data show an approximately twofold increase in malonyldialdehyde levels ($P < 0.01$) in the cardiac mitochondria of infected mice (Figure 3B, Table 1). Similarly, a substantial increase in DNP-derivatized protein carbonyls was noted in the cardiac mitochondria of infected mice (Figure 3C). PBN treatment resulted in complete inhibition of mitochondrial malonyldialdehyde deposition ($P < 0.01$; Figure 3B, Table 1). The extent of protein carbonylation in cardiac mitochondria of infected/PBN-treated mice, although higher than that detected in normal controls, was also considerably decreased compared with findings in infected/untreated mice (Figure 3C). The inhibition of mitochondrial lipid and protein oxidation was associated with preservation of the mitochondrial membranes in PBN-treated/infected mice (Figure 3A, compare IPBNT versus IUT). These data suggest that oxidative stress contributes to mitochondrial morphological alterations in infected mice and that PBN treatment was effective in arresting the ROS-elicited oxidation of mitochondrial membranes and in preserving the mitochondrial integrity in acutely infected mice.

ROS-mediated oxidative modifications of mtDNA result in rapid degradation of damaged DNA and mtDNA depletion.[22] Given that mtDNA encodes essential subunits of the respiratory complexes, depletion of mtDNA can result in limited expression and assembly of the respiratory complexes. We examined the mtDNA content in infected mice by Southern blot analysis using mtDNA-specific *CO2* probe. We observed no statistically significant change in mtDNA levels in infected and PBN-treated mice compared with that detected in normal controls (data not shown). The mtDNA-specific *CO2* and *ND1*, and nDNA-specific *GAPDH* genes were amplified at a similar efficiency in real-time PCR with cardiac DNA isolated from infected, infected/PBN-treated, and normal controls (data not shown), thus confirming the results of Southern blot analysis. These data suggest that mtDNA depletion is not a major mechanism in respiratory complex deficiencies in infected mice.

Despite no alteration in mtDNA content, oxidation of mitochondrial membranes altering the membrane integrity and redox potential can affect coupled mitochondrial gene expression, and subsequently, contribute to respiratory complex deficiencies.[45,46] We, therefore, measured the level of transcripts for mitochondria-encoded subunits of the respiratory complexes by Northern blot analysis (Figure 4A). Intensity of bands for mitochondria-encoded transcripts was determined by densitometric analysis and normalized to rRNA content. Our data show in infected murine myocardium a 58%, 60 to 62%, and 61 to 65% decline in mitochondria-encoded transcripts for ND4L, CO1/CO2, and ATP6/ATP8 subunits of the CI, CIV, and CV respiratory complexes, respectively. PBN treatment normalized the expression level of transcripts for

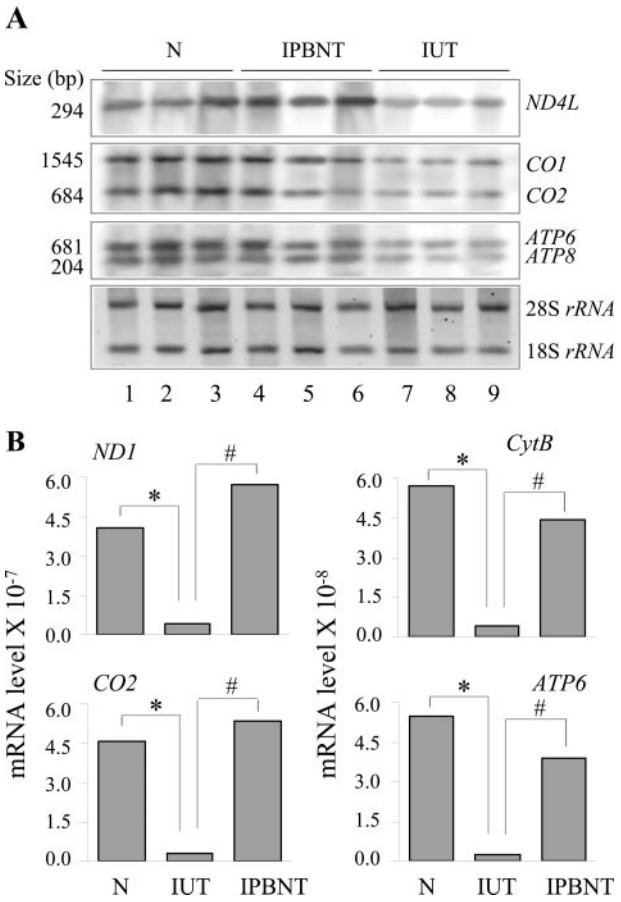

Figure 4. mtRNA in *T. cruzi*-infected (±PBN) murine hearts. Northern blotting. Cardiac total RNA was resolved by denaturing agarose gel electrophoresis and then transferred to a nylon membrane. **A:** Northern blot analysis was performed with ^{32}P-labeled, mitochondria-specific cDNA probes. Phosphorimages of mitochondria-encoded transcripts were quantitated by densitometric analysis and normalized to the amounts of 18S rRNA. Real-time RT-PCR. Total RNA was reverse-transcribed to synthesize first-strand cDNA and subsequently used as a template with gene-specific primer pairs. **B:** Results were normalized to GAPDH. $1/2^{Ct}$ values, representative of mRNA expression levels are plotted on the *y* axis. The SD for all of the data points was <5%. Data are representative of two independent experiments ($n = 3$ mice/experiment/group). $^{*\#}P < 0.05$.

ND4L and resulted in 76 to 77% and 89 to 94% gain in mRNAs for CO1/CO2 and ATP6/ATP8 subunits, respectively, as compared with that in infected/untreated mice (Figure 4A). Results of Northern blotting were confirmed by real-time RT-PCR analysis. For each target gene, the threshold cycle (C_t) values, representative of mRNA expression level, were normalized to *GAPDH* expression. The *ND1*, *CYT B*, *CO2*, and *ATP6* mRNAs for the CI, CIII, CIV, and CV respiratory complex subunits, respectively, were decreased by ≥85% in infected murine hearts when compared with that detected in normal controls. The expression level of these transcripts in PBN-treated infected mice was restored to near normal level (Figure 4B). These data show that PBN arrested the loss of mtDNA-encoded transcripts in infected mice.

Finally, oxidation of specific subunits of the respiratory complexes is shown to result in inactivation of the complex enzymatic activities.[14] PBN may limit the oxidative damage of respiratory complexes. We resolved the respiratory complexes by two-dimensional BN-PAGE and

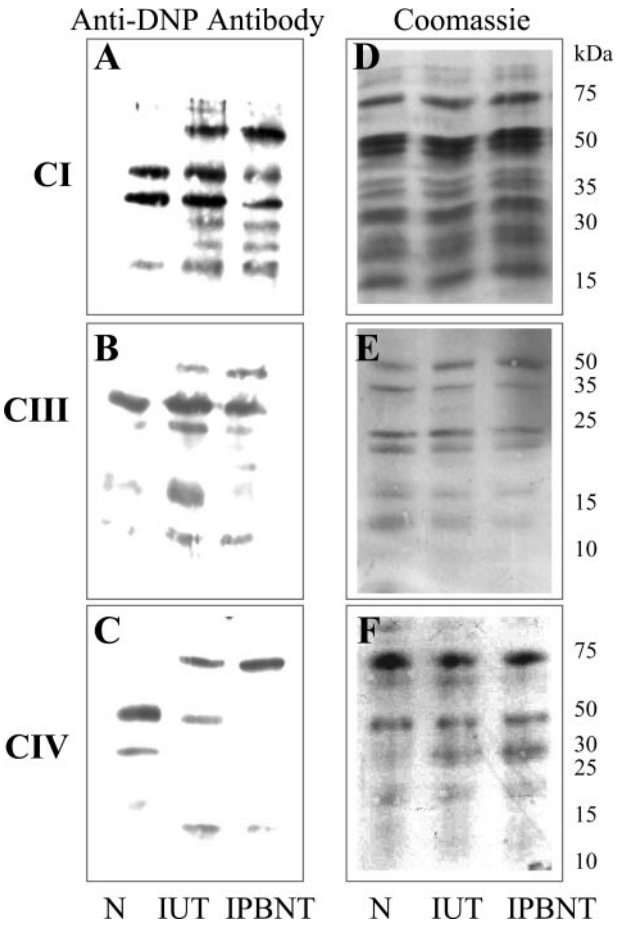

Figure 5. Carbonylation of respiratory complex subunits in cardiac mitochondria of infected (±PBN) mice. Myocardial mitochondria were solubilized and the subunits of CI, CIII, and CIV respiratory chain complexes resolved by two-dimensional BN-PAGE. **A–C:** The oxidatively modified proteins were detected by immunoblotting with anti-DNP antibody. **D–F:** Coomassie blue stains of the membranes used for immunoblot analysis are shown. Data are representative of two independent experiments ($n = 3$ mice/group).

determined the extent of oxidative carbonylation by Western blot analysis with anti-DNP antibody. As shown in Figure 5, A–C, cardiac mitochondria of infected mice incurred a substantial oxidation of several subunits of the respiratory complexes compared with normal controls, also noted in a previous study.[14] PBN treatment resulted in a marginal decrease in oxidation of respiratory complex subunits in infected mice (Figure 5, A–C). Coomassie blue staining of the membranes used for immunoblot analysis with anti-DNP antibody confirmed equal loading of the protein samples (Figure 5, D–F). Our data suggest that PBN has limited efficacy in neutralizing the oxidative modifications of assembled respiratory complexes in the cardiac mitochondria of infected mice.

PBN Normalized the Cellular Antioxidant Status in Infected Mice

Mammalian cells use different antioxidant defenses to cope with oxidative stress.[47–49] Previously, we have shown that infected mice failed to elicit the antioxidant defense that is sufficient to counterbalance the myocardial oxidative stress.[38] In agreement with published results, in this study, we noted a substantial decline in the expression level of mRNAs for the SOD1, SOD2, GPx, and CAT antioxidants in the infected murine hearts. On PBN treatment, the mRNA level for the antioxidant enzymes in the infected mice were normalized to that detected in wild-type controls (data not shown). The endogenous level of GSH is an important biomarker of host antioxidant status. In agreement with the steady expression of antioxidant genes, PBN-treated/infected mice exhibited normalized GSH level. The GSH contents in infected/untreated mice were decreased by 24% compared with that detected in normal controls and PBN-treated/infected mice (Table 1). These data, along with that presented in Figure 6, suggest that antioxidant status is compromised in infected murine hearts and that PBN treatment stabilized the cellular antioxidant status in infected mice but did not alter the host capacity to control *T. cruzi*.

Host Protective Responses against T. cruzi *Were Not Altered by PBN*

The host immune mechanisms control *T. cruzi* through activation of cytotoxic agents, ie, ROS and reactive nitrogen species.[50–53] The treatment with an antioxidant PBN may restrain the immune-mediated parasite control, thereby exacerbating the parasite burden in the heart tissue. We performed *T. cruzi* rDNA-specific semiquantitative PCR to evaluate the tissue parasite burden in infected mice. Our data show similar amplification of *T. cruzi* rDNA in infected/untreated and PBN-treated/infected murine hearts (Figure 6A). No statistically significant differences were observed in β-actin normalized *T. cruzi* rDNA in infected (±PBN) mice (Figure 6B). Specificity of the PCR reaction was confirmed by no amplification of the parasite rDNA on incubation of *T. cruzi* or infected mouse DNA with one primer (data not shown) or normal mouse DNA with both the primers (Figure 6A). Histological analysis of tissue sections revealed parasite foci in the heart tissue of infected and PBN-treated/infected mice (Figure 6C). Infiltration of inflammatory cells either closely associated with the parasitic lesions or diffused throughout the tissue was noticeable in the myocardium of acutely infected mice, and remained unaltered by PBN treatment (Figure 6C). Further, we observed no effect of PBN treatment on increased cellular levels of H_2O_2 (Figure 6D, Table 1) in infected murine hearts. These data show that PBN did not alter the host protective responses against *T. cruzi* infection.

Discussion

The present study shows that cardiac mitochondrial decay is evidenced by decreased respiratory complex activities, inefficiency of the electron transport chain, increased ROS generation, and diminished energy (ATP) levels during acute *T. cruzi* infection. Many of these al-

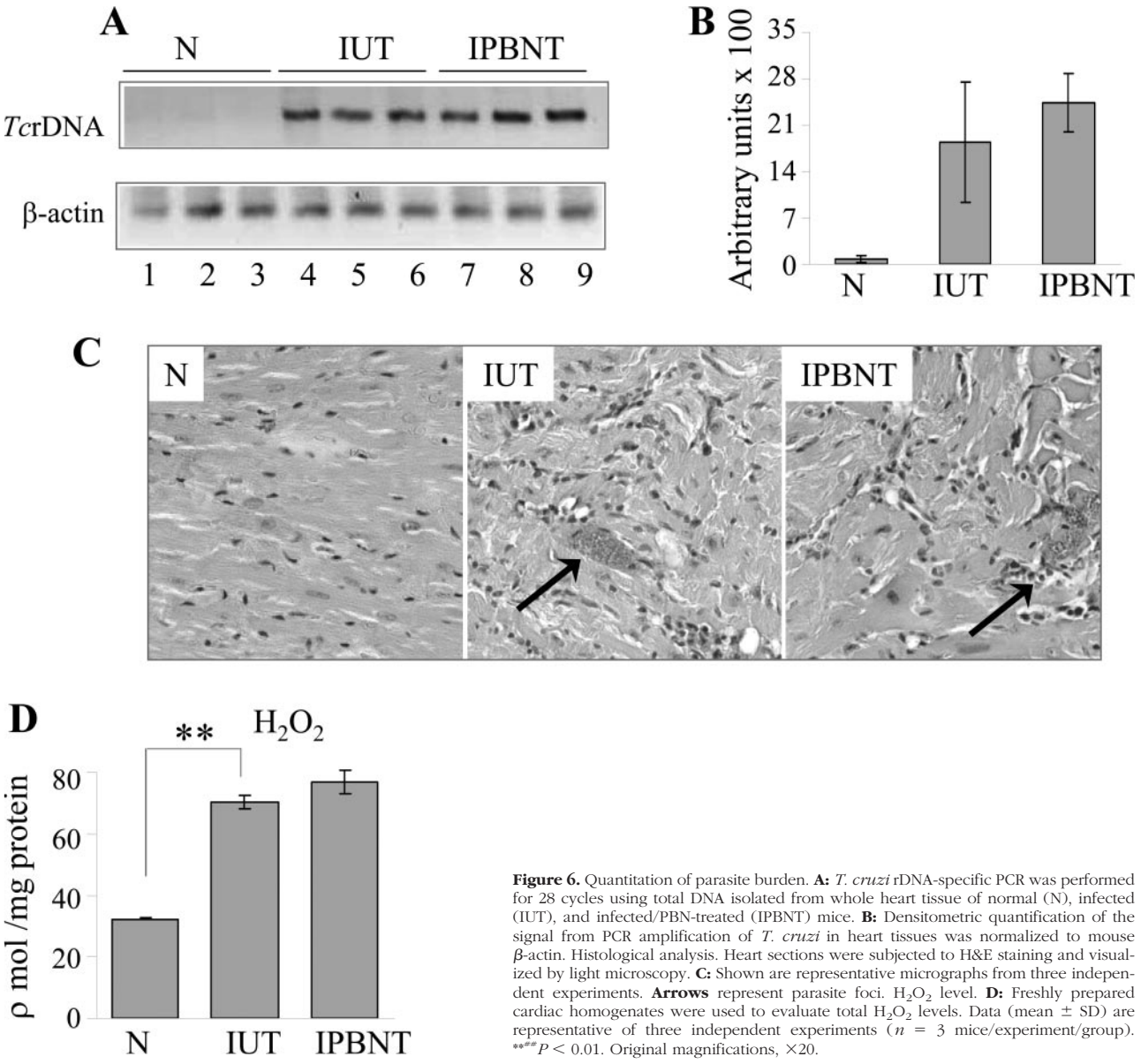

Figure 6. Quantitation of parasite burden. **A:** *T. cruzi* rDNA-specific PCR was performed for 28 cycles using total DNA isolated from whole heart tissue of normal (N), infected (IUT), and infected/PBN-treated (IPBNT) mice. **B:** Densitometric quantification of the signal from PCR amplification of *T. cruzi* in heart tissues was normalized to mouse β-actin. Histological analysis. Heart sections were subjected to H&E staining and visualized by light microscopy. **C:** Shown are representative micrographs from three independent experiments. **Arrows** represent parasite foci. H_2O_2 level. **D:** Freshly prepared cardiac homogenates were used to evaluate total H_2O_2 levels. Data (mean ± SD) are representative of three independent experiments (n = 3 mice/experiment/group). $^{**\#\#}P < 0.01$. Original magnifications, ×20.

tered characteristics of mitochondrial metabolism were reversed by PBN treatment of infected mice. The beneficial effects of PBN in restoring mitochondrial function and energy output were associated with an inhibition of mitochondrial oxidative damage. This is the first study to demonstrate the pathological significance of oxidative modifications of cardiac mitochondria in metabolic decay and energy homeostasis in acute chagasic myocarditis.

We have shown that respiratory complex activities and electron transport chain efficiency were substantially diminished during acute chagasic myocarditis and resulted in decreased availability of metabolic energy (ATP) in the myocardium. Treatment of infected mice with PBN, an antioxidant, arrested the mitochondrial oxidative damage (Figure 3, B and C) and subsequently improved the respiratory complex activities (Figure 1) and tissue ATP levels (Figure 2, A and B). These observations, along with our previous studies,[8,14,38] allow us to propose that oxidative stress causes mitochondrial decay in *T. cruzi*-infected myocardium. Trapping the free radicals and reactive intermediates or inhibiting the free radical-producing reactions would be beneficial in interrupting the mitochondrial functional decline and preserving the cardiac energy status in acutely infected mice. This notion is supported by others who have demonstrated the efficacy of PBN in arresting the age-dependent decay of cellular respiration, mitochondrial membrane potential, and aconitase activity in *in vitro* cultured cells[54,55] and in maintaining the mitochondrial bioenergetic status in the brain of experimental animals with ongoing seizure.[56]

What might be the source of oxidative stress causing mitochondrial decay in the infected murine myocardium is not clear. Others have shown that a low but constant production of free radicals ($O_2^{\cdot-}$ and H_2O_2) occurs in mitochondria because of unavoidable leakage of electrons from electron transport chain to O_2.[11] A substantial de-

cline in the respiratory chain complex activities, as noted in acutely infected murine hearts (Figure 1), is likely to result in increased release of electrons to molecular O_2 and thus to augment ROS production in cardiac mitochondria. Consequently, we have shown a substantial increase in H_2O_2 content and H_2O_2 release rate in cardiac mitochondria of infected mice (Figure 3, C and D). In addition to endogenous ROS, oxidative stress of inflammatory origin may also cause mitochondrial decay in chagasic myocardium. Numerous studies have documented that acute *T. cruzi* infection elicits proinflammatory cytokines that augment NO production and oxidative burst in a host.[9,57,58] The efficacy of PBN in preventing mitochondrial decay in infected mice was associated with preservation of respiratory chain efficiency and a substantial decline in mtROS release. PBN was, however, ineffective in scavenging cellular ROS in infected myocardium (Figure 6D, Table 1). These data provide evidence that enhanced mtROS release attributable to respiratory chain deficiency and not the cellular ROS, is the prime cause for oxidative stress-mediated mitochondrial injuries in infected murine myocardium. The importance of these observations lays in the fact that inhibition of mitochondrial respiratory complexes and enhanced ROS release, a self-perpetuating process, would result in increasing order of mitochondrial functional decline and energy depletion with progression of chagasic cardiomyopathy. Antioxidant treatment would likely be effective in controlling sustained mitochondrial decay in Chagas' disease.

Concerning the oxidative stress-mediated mechanisms that contribute to mitochondrial functional decline and may be altered by PBN, it is noted that mitochondrial respiratory complexes, being the site of ROS release, are in close proximity to mtROS and are highly susceptible to oxidative stress. The oxidative modifications may affect the processing and/or folding of the proteins[59] resulting in inactivation of the respiratory complexes. We have previously shown 4-hydroxy-2-nonenal-mediated oxidative adduct formation result in catalytic inactivation of the assembled respiratory complexes.[14] The data presented in this study show that despite a decline in mtROS release (Figure 3, C and D), PBN-treated/infected mice exhibited a similar level of oxidative modification of respiratory complexes as was detected in the myocardium of infected/untreated mice (Figure 5, A and C). These data imply the beneficial effects of PBN in enhancing the electron transport chain efficiency and energy output in infected murine myocardium were not delivered through prevention of ROS-mediated inactivation of assembled complexes.

Importantly, infected mice given PBN exhibited minimal oxidation of mitochondrial membranes. Oxidation of mitochondrial membrane phospholipids and proteins in infected murine hearts, as noted in this and other reports,[14] alters membrane integrity and fluidity and affects redox potential essential for coupled mitochondrial gene expression.[45] Our data demonstrate that alteration in mitochondrial morphology (Figure 3A) and oxidation of mitochondrial membranes in infected myocardium (Figure 3, B and C) corresponded with a substantial decline in mitochondria-encoded transcripts (Figure 4). Infected/PBN-treated mice, capable of arresting the mitochondrial membrane oxidation and the alteration in mitochondrial morphology (Figure 3A), exhibited improved expression of mitochondrial mRNAs (Figure 4) and, subsequently, restored respiratory complex activities (Figure 1) and energy status (Figure 2, A and B). It is likely that the lipophilic nature of PBN allowed it to reach the highly oxidation-susceptible polyunsaturated fatty acids in the lipid bilayer, where phenolic head group of PBN scavenged the free radicals while lipophilic side chains aligned with the lipid fatty acids, thus offering membrane stability and preservation of the structure and integrity of mitochondria.

It is well documented that ROS and reactive nitrogen species of inflammatory origin play an important role in killing *T. cruzi* in the host.[51–53] Treatment with an antioxidant resulting in scavenging of cellular reactive species may exacerbate parasite survival and replication. We have observed statistically insignificant differences in the myocardial level of inflammatory infiltrate, cytotoxic agents (H_2O_2) in infected and infected/PBN-treated mice (Figure 6, data not shown). Subsequently, parasite burden in the myocardium of PBN-treated/infected mice was similar to that detected in infected/untreated mice (Figure 6A). These data demonstrate that PBN has no deleterious effects on the host's ability to kill *T. cruzi* via activation of immune mechanisms.

In conclusion, we have shown that acute Chagas' disease is accompanied by inefficiency of respiratory complexes resulting in a decline in energy (ATP) level and increased ROS release in cardiac mitochondria. These metabolic alterations were associated with free radical-mediated oxidative insult of mitochondria and reversed by PBN. Specifically, PBN arrested the oxidative damage-mediated loss in mitochondrial membrane integrity, preserved redox potential coupled mitochondrial gene expression, and improved respiratory complex activities in infected myocardium. Importantly, PBN-mediated normalization of respiratory complex activities led to inhibition of a feedback cycle of electron transport chain inefficiency, increased ROS production, and energy homeostasis in acute chagasic hearts. We propose that antioxidants (eg, PBN) capable of modulating or delaying the onset of oxidative insult and mitochondrial deficiencies in the myocardium would prove to be useful in preserving cardiac functions in the acute Chagas' disease. Future studies addressing the effect of PBN and mitochondria-targeted antioxidants in altering the mitochondrial decay and oxidative pathology, once they are initiated and sustained, as in chronic Chagas' disease, are warranted.

Acknowledgments

We thank Dr. John Papaconstantinou for providing the plasmids encoding mitochondrial subunits, Dr. Istvan Boldogh for constructive discussions, and Ms. Mardelle Susman for editing and proofreading the manuscript.

References

1. World Health Organization: Control of Chagas Disease: WHO Technical Report Series 905. Second Report of the WHO Expert Committee. Geneva, Switzerland, 2002, pp 1–99
2. Carrasco Guerra HA, Palacios-Pru E, Dagert de Scorza C, Molina C, Inglessis G, Mendoza RV: Clinical, histochemical, and ultrastructural correlation in septal endomyocardial biopsies from chronic chagasic patients: detection of early myocardial damage. Am Heart J 1987, 113:716–724
3. Palacios-Pru E, Carrasco H, Scorza C, Espinoza R: Ultrastructural characteristics of different stages of human chagasic myocarditis. Am J Trop Med Hyg 1989, 41:29–40
4. Parada H, Carrasco HA, Anez N, Fuenmayor C, Inglessis I: Cardiac involvement is a constant finding in acute Chagas' disease: a clinical, parasitological and histopathological study. Int J Cardiol 1997, 60:49–54
5. Garg N, Popov VL, Papaconstantinou J: Profiling gene transcription reveals a deficiency of mitochondrial oxidative phosphorylation in Trypanosoma cruzi-infected murine hearts: implications in chagasic myocarditis development. Biochim Biophys Acta 2003, 1638:106–120
6. Uyemura SA, Albuquerque S, Curti C: Energetics of heart mitochondria during acute phase of Trypanosoma cruzi infection in rats. Int J Biochem Cell Biol 1995, 27:1183–1189
7. Uyemura SA, Jordani MC, Polizello AC, Curti C: Heart FoF1-ATPase changes during the acute phase of Trypanosoma cruzi infection in rats. Mol Cell Biochem 1996, 165:127–133
8. Vyatkina G, Bhatia V, Gerstner A, Papaconstantinou J, Garg N: Impaired mitochondrial respiratory chain and bioenergetics during chagasic cardiomyopathy development. Biochim Biophys Acta 2004, 1689:162–173
9. Brener Z, Gazzinelli RT: Immunological control of Trypanosoma cruzi infection and pathogenesis of Chagas' disease. Int Arch Allergy Immunol 1997, 114:103–110
10. Turrens JF: Oxidative stress and antioxidant defenses: a target for the treatment of diseases caused by parasitic protozoa. Mol Aspects Med 2004, 25:211–220
11. Turrens JF: Mitochondrial formation of reactive oxygen species. J Physiol 2003, 552:335–344
12. Ide T, Tsutsui H, Kinugawa S, Utsumi H, Kang D, Hattori N, Uchida K, Arimura K, Egashira K, Takeshita A: Mitochondrial electron transport complex I is a potential source of oxygen free radicals in the failing myocardium. Circ Res 1999, 85:357–363
13. Chen Q, Vazquez EJ, Moghaddas S, Hoppel CL, Lesnefsky EJ: Production of reactive oxygen species by mitochondria: central role of complex III. J Biol Chem 2003, 278:36027–36031
14. Wen J-J, Garg N: Oxidative modifications of mitochondrial respiratory complexes in response to the stress of Trypanosoma cruzi infection. Free Radic Biol Med 2004, 37:2072–2081
15. Fernandez-Moreno MA, Bornstein B, Petit N, Garesse R: The pathophysiology of mitochondrial biogenesis: towards four decades of mitochondrial DNA research. Mol Genet Metab 2000, 71:481–495
16. Kelly DP, Scarpulla RC: Transcriptional regulatory circuits controlling mitochondrial biogenesis and function. Genes Dev 2004, 18:357–368
17. Evans MD, Cooke MS: Factors contributing to the outcome of oxidative damage to nucleic acids. Bioessays 2004, 26:533–542
18. Yu H, Liu J, Li J, Zang T, Luo G, Shen J: Protection of mitochondrial integrity from oxidative stress by selenium-containing glutathione transferase. Appl Biochem Biotechnol 2005, 127:133–142
19. Manczak M, Park BS, Jung Y, Reddy PH: Differential expression of oxidative phosphorylation genes in patients with Alzheimer's disease: implications for early mitochondrial dysfunction and oxidative damage. Neuromol Med 2004, 5:147–162
20. Vercesi AE, Kowaltowski AJ, Grijalba MT, Meinicke AR, Castilho RF: The role of reactive oxygen species in mitochondrial permeability transition. Biosci Rep 1997, 17:43–52
21. Cardoso SM, Pereira C, Oliveira R: Mitochondrial function is differentially affected upon oxidative stress. Free Radic Biol Med 1999, 26:3–13
22. Wei YH, Lu CY, Lee HC, Pang CY, Ma YS: Oxidative damage and mutation to mitochondrial DNA and age-dependent decline of mitochondrial respiratory function. Ann NY Acad Sci 1998, 854:155–170
23. Palmeira CM, Serrano J, Kuehl DW, Wallace KB: Preferential oxidation of cardiac mitochondrial DNA following acute intoxication with doxorubicin. Biochim Biophys Acta 1997, 1321:101–106
24. Williams MD, Van Remmen H, Conrad CC, Huang TT, Epstein CJ, Richardson A: Increased oxidative damage is correlated to altered mitochondrial function in heterozygous manganese superoxide dismutase knockout mice. J Biol Chem 1998, 273:28510–28515
25. Serrano J, Palmeira CM, Kuehl DW, Wallace KB: Cardioselective and cumulative oxidation of mitochondrial DNA following subchronic doxorubicin administration. Biochim Biophys Acta 1999, 1411:201–205
26. Floyd RA, Hensley K, Forster MJ, Kelleher-Anderson JA, Wood PL: Nitrones as neuroprotectants and antiaging drugs. Ann NY Acad Sci 2002, 959:321–329
27. Kotake Y: Pharmacologic properties of phenyl N-tert-butylnitrone. Antioxid Redox Signal 1999, 1:481–499
28. Plata F, Garcia Pons F, Eisen H: Antigenic polymorphism of Trypanosoma cruzi: clonal analysis of trypomastigote surface antigens. Eur J Immunol 1984, 14:392–399
29. Chomczynski P, Sacchi N: Single-step method of RNA isolation by acid guanidinium thiocyanate-phenol-chloroform extraction. Anal Biochem 1987, 162:156–159
30. Saito H, Patterson C, Hu Z, Runge MS, Tipnis U, Sinha M, Papaconstantinou J: Expression and self-regulatory function of cardiac interleukin-6 during endotoxemia. Am J Physiol 2000, 279:H2241–H2248
31. Sharma S, Dewald O, Adrogue J, Salazar RL, Razeghi P, Crapo JD, Bowler RP, Entman ML, Taegtmeyer H: Induction of antioxidant gene expression in a mouse model of ischemic cardiomyopathy is dependent on reactive oxygen species. Free Radic Biol Med 2006, 40:2223–2231
32. Garg N, Bhatia V, Gerstner A, DeFord J, Papaconstantinou J: Gene expression analysis in mitochondria from chagasic mice: alterations in specific metabolic pathways. Biochem J 2004, 381:743–752
33. Jarreta D, Orus J, Barrientos A, Miro O, Roig E, Heras M, Moraes CT, Cardellach F, Casademont J: Mitochondrial function in heart muscle from patients with idiopathic dilated cardiomyopathy. Cardiovasc Res 2000, 45:860–865
34. Bradford MA: A rapid and sensitive method for quantitation of microgram quantities of protein utilizing the principle of protein-DNA binding. Anal Biochem 1976, 72:248–254
35. Schagger H: Native electrophoresis for isolation of mitochondrial oxidative phosphorylation protein complexes. Methods Enzymol 1995, 260:190–202
36. Zerbetto E, Vergani L, Dabbeni-Sala F: Quantification of muscle mitochondrial oxidative phosphorylation enzymes via histochemical staining of blue native polyacrylamide gels. Electrophoresis 1997, 18:2059–2064
37. Ohkawa H, Ohishi N, Yagi K: Assay for lipid peroxides in animal tissues by thiobarbituric acid reaction. Anal Biochem 1979, 95:351–358
38. Wen J-J, Vyatkina G, Garg N: Oxidative damage during chagasic cardiomyopathy development: role of mitochondrial oxidant release and inefficient antioxidant defense. Free Radic Biol Med 2004, 37:1821–1833
39. Levine RL, Garland D, Oliver CN, Amici A, Climent I, Lenz AG, Ahn BW, Shaltiel S, Stadtman ER: Determination of carbonyl content in oxidatively modified proteins. Methods Enzymol 1990, 186:464–478
40. Tietze F: Enzymic method for quantitative determination of nanogram amounts of total and oxidized glutathione: applications to mammalian blood and other tissues. Anal Biochem 1969, 27:502–522
41. Wen J-J, Yachelini PC, Sembaj A, Manzur RE, Garg N: Increased oxidative stress is correlated with mitochondrial dysfunction in chagasic patients. Free Radic Biol Med 2006, 41:270–276
42. Wibom R, Lundin A, Hultman E: A sensitive method for measuring ATP-formation in rat muscle mitochondria. Scand J Clin Lab Invest 1990, 50:143–152
43. Sun J, Tarleton RL: Predominance of CD8+ T lymphocytes in the inflammatory lesions of mice with acute Trypanosoma cruzi infection. Am J Trop Med Hyg 1993, 48:161–169
44. Garg N, Tarleton RL: Genetic immunization elicits antigen-specific protective immune responses and decreases disease severity in Trypanosoma cruzi infection. Infect Immun 2002, 70:5547–5555
45. Berdanier CD: Mitochondrial gene expression in diabetes mellitus: effect of nutrition. Nutr Rev 2001, 59:61–70
46. Aleardi AM, Benard G, Augereau O, Malgat M, Talbot JC, Mazat JP,

Letellier T, Dachary-Prigent J, Solaini GC, Rossignol R: Gradual alteration of mitochondrial structure and function by beta-amyloids: importance of membrane viscosity changes, energy deprivation, reactive oxygen species production, and cytochrome c release. J Bioenerg Biomembr 2005, 37:207–225
47. Kurata M, Suzuki M, Agar NS: Antioxidant systems and erythrocyte life-span in mammals. Comp Biochem Physiol B 1993, 106:477–487
48. Nordberg J, Arner ES: Reactive oxygen species, antioxidants, and the mammalian thioredoxin system. Free Radic Biol Med 2001, 31:1287–1312
49. Dickinson DA, Forman HJ: Glutathione in defense and signaling: lessons from a small thiol. Ann NY Acad Sci 2002, 973:488–504
50. Schirmer RH, Schollhammer T, Eisenbrand G, Krauth-Siegel RL: Oxidative stress as a defense mechanism against parasitic infections. Free Radic Res Commun 1987, 3:3–12
51. Lima EC, Garcia I, Vicentelli MH, Vassalli P, Minoprio P: Evidence for a protective role of tumor necrosis factor in the acute phase of Trypanosoma cruzi infection in mice. Infect Immun 1997, 65:457–465
52. Munoz-Fernandez MA, Fernandez MA, Fresno M: Synergism between tumor necrosis factor-alpha and interferon-gamma on macrophage activation for the killing of intracellular Trypanosoma cruzi through a nitric oxide-dependent mechanism. Eur J Immunol 1992, 22:301–307
53. Cardoni RL, Antunez MI, Morales C, Nantes IR: Release of reactive oxygen species by phagocytic cells in response to live parasites in mice infected with Trypanosoma cruzi. Am J Trop Med Hyg 1997, 56:329–334
54. Hagen TM, Wehr CM, Ames BN: Mitochondrial decay in aging. Reversal through supplementation of acetyl-L-carnitine and N-tert-butyl-alpha-phenyl-nitrone. Ann NY Acad Sci 1998, 854:214–223
55. Atamna H, Paler-Martinez A, Ames BN: N-t-butyl hydroxylamine, a hydrolysis product of alpha-phenyl-N-t-butyl nitrone, is more potent in delaying senescence in human lung fibroblasts. J Biol Chem 2000, 275:6741–6748
56. Folbergrova J, He QP, Li PA, Smith ML, Siesjo BK: The effect of alpha-phenyl-N-tert-butyl nitrone on bioenergetic state in substantia nigra following flurothyl-induced status epilepticus in rats. Neurosci Lett 1999, 266:121–124
57. Martins GA, Cardoso MA, Aliberti JC, Silva JS: Nitric oxide-induced apoptotic cell death in the acute phase of Trypanosoma cruzi infection in mice. Immunol Lett 1998, 63:113–120
58. Zacks MA, Wen J-J, Vyatkina G, Bhatia V, Garg N: An overview of chagasic cardiomyopathy: pathogenic importance of oxidative stress. Ann Acad Bras Cienc 2005, 77:695–715
59. Rakhit R, Cunningham P, Furtos-Matei A, Dahan S, Qi XF, Crow JP, Cashman NR, Kondejewski LH, Chakrabartty A: Oxidation-induced misfolding and aggregation of superoxide dismutase and its implications for amyotrophic lateral sclerosis. J Biol Chem 2002, 277:47551–47556